



**HAL**  
open science

## Perception of loudness changes induced by a phononic crystal in specific frequency bands

Arthur Paté, Nicolas Côté, Charles Croënne, Jerome O. Vasseur,  
Anne-Christine Hladky-Hennion

► **To cite this version:**

Arthur Paté, Nicolas Côté, Charles Croënne, Jerome O. Vasseur, Anne-Christine Hladky-Hennion. Perception of loudness changes induced by a phononic crystal in specific frequency bands. *Acta Acustica*, 2022, 6, pp.42. 10.1051/aacus/2022037 . hal-03789110

**HAL Id: hal-03789110**

**<https://hal.science/hal-03789110v1>**

Submitted on 27 Sep 2022

**HAL** is a multi-disciplinary open access archive for the deposit and dissemination of scientific research documents, whether they are published or not. The documents may come from teaching and research institutions in France or abroad, or from public or private research centers.





L'archive ouverte pluridisciplinaire **HAL**, est destinée au dépôt et à la diffusion de documents scientifiques de niveau recherche, publiés ou non, émanant des établissements d'enseignement et de recherche français ou étrangers, des laboratoires publics ou privés.



Distributed under a Creative Commons Attribution 4.0 International License



# Perception of loudness changes induced by a phononic crystal in specific frequency bands

Arthur Paté<sup>1,\*</sup> , Nicolas Côté<sup>2</sup>, Charles Croënne<sup>1</sup> , Jérôme Vasseur<sup>1</sup> , and Anne-Christine Hladky-Hennion<sup>1</sup> 

<sup>1</sup> Univ. Lille, CNRS, Centrale Lille, Univ. Polytechnique Hauts-de-France, Junia, UMR 8520 – IEMN, 59000 Lille, France

<sup>2</sup> Wavely SAS, 4 rue Archimède, 59650 Villeneuve-d'Ascq, France

Received 20 September 2021, Accepted 25 August 2022

**Abstract** – To study the influence of classical phononic crystal (PC) structures on the acoustical characteristics of a sound source, a combined acoustics/perceptual analysis is conducted on a PC specially designed to exhibit several spectral and wave vector properties in different audible frequency ranges. The properties, confirmed by both numerical calculations and experiments, consist in both partial and absolute band gaps, as well as a negative refraction band. A psychoacoustic feature, namely the loudness in third-octave bands, is estimated from numerical simulations of the acoustic field behind the crystal. Additional perceptual tests are conducted to evaluate the efficiency of the PC slab. In the frequency range of the band gaps, sound stimuli filtered by the PC's impulse response are perceived as softer than stimuli resulting from a free-field propagation (FF), they also are perceived as equally (or close to equally) loud than sounds attenuated by a free-standing rigid wall (FS). In the frequency range of the focalization (negative refraction), PC sound stimuli sound louder than both FS and FF sound stimuli. The possibility of designing an efficient sound barrier based on the considered PC is finally discussed.

**Keywords:** Phononic crystals, Band gaps, Sound attenuation, Loudness, Sound barrier

## 1 Introduction

Within the last decades, phononic crystals (PCs), defined as artificial elastic composite materials exhibiting a periodic structure [1, 2], have received a great deal of attention. Bragg scattering in such periodic structures may lead to unusual spectral and wave vector properties that cannot be observed in common materials. One can mention the existence, under certain conditions (geometry of the array of inclusions, filling factor of inclusions, inclusion shape, etc.), of band-gaps in the frequency versus wave number diagram, where the propagation of acoustic waves is forbidden. Such band gaps are either absolute, i.e. the waves are evanescent whatever the incidence angle (named Absolute Band Gap, ABG) or for some specific angle, for example the normal incidence (named Band Gap  $0^\circ$ , BG $0^\circ$ ). These spectral properties confer to PCs potential applications in various fields such as sound insulation, selective frequency filtering, waveguiding or for the realization of more efficient transducers for nondestructive control or medical imaging [3].

Wave-vector properties of PCs are associated with pass bands that possess very peculiar shapes. For example, a negative refraction phenomenon occurs when some band

presents a negative slope in a specific frequency range in the frequency vs. wave number diagram. In this case, the phase and group velocity vectors have opposite orientations and the sound waves are refracted with a negative angle at the interface between the PC and its surrounding medium. In other words, in this specific frequency range, the PC behaves as an effective medium with a negative index of refraction [4]. Moreover, when the index of refraction of the PC takes a negative value and its absolute value is equal to that of the surrounding medium for all incidence angles, one may observe a focalization of the waves (all-angle negative refraction criterion): a point source located in front of one side of a PC slab gives a point image on the other side of the slab. The distance between the point source and the image point was shown to be twice as large as the PC slab thickness [5, 6].

While numerous studies on PCs were focused on the characterization of these structures in terms of band gaps and refraction phenomena [3], less work has been done on the analysis in the audible frequency range, and on the perception of these wave phenomena by a listener, except a preliminary study on a perceptual evaluation of metamaterials [7]. One may also cite the works by Spiouzas et al. [8, 9] where the authors study the influence of a PC on the auditory distance perception of sound sources. Results of their auditory test show that negative refraction in PCs may

\*Corresponding author: [arthur.pate@isen.fr](mailto:arthur.pate@isen.fr)

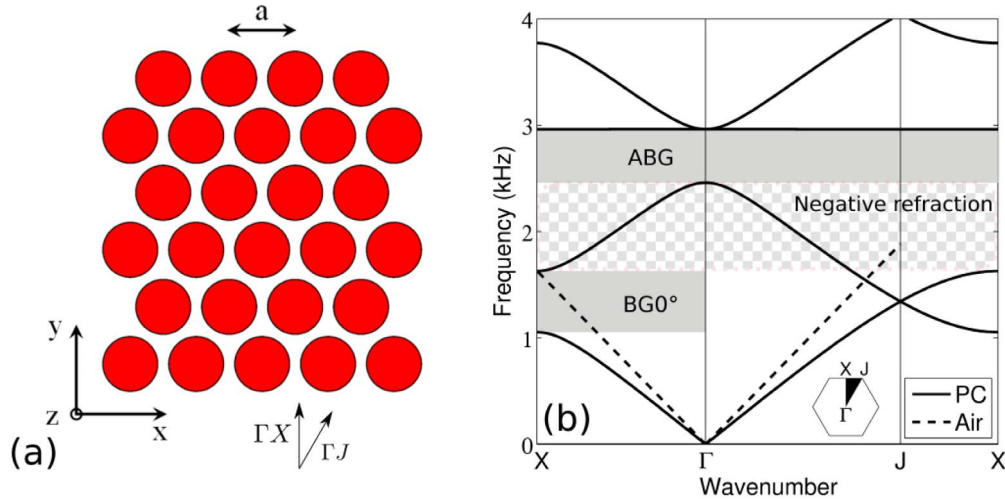


**Figure 1.** (a) Transverse cross section in the  $xy$ -plane of the PC made of a triangular array of solid cylinders surrounded with air. Thin arrows indicate the directions of propagation  $\Gamma J$  and  $\Gamma X$ . (b) Dispersion curves of the PC. The ABG and the band gap for normal incidence ( $BG0^\circ$ ) are shown in gray, and the negative refraction band is shown by the white and gray checkerboard area. Inset: full and reduced Brillouin zones for the triangular lattice, showing the definition of the labels for the symmetry points (see text for details). The dashed line represent the dispersion curve in the air, i.e. when no dispersion occurs ( $f = \frac{kc_{\text{air}}}{2\pi}$ , with  $f$  the frequency,  $k$  the wave number, and  $c_{\text{air}}$  the speed of sound in the air), along both principal directions of propagation  $\Gamma J$  and  $\Gamma X$ .

artificially make a sound source appear closer to the listener. Moreover, it was also shown that a sonic crystal placed between a musician and the audience is able to greatly modify the timbre and directivity pattern of an instrument during the performance [10].

The aim of this paper is to assess whether a PC slab introduces auditory effects on the sound emitted by a source. Are the spectral content and loudness of the source altered by the PC within the frequency bands of the typical effects related to a PC (band gaps, focalization)? Can these alterations eventually be heard by listeners?

This paper presents a combined acoustical/perceptual study of the effects induced by a PC slab on the propagation of acoustic waves. Section 2 describes the studied PC and reports on theoretical results obtained with the finite element method (FEM). It is shown that the structure of interest exhibits three different propagation phenomena in three different frequency ranges: namely, a band gap at normal incidence, an ABG irrespective of the direction of propagation of incident waves and a negative refraction of incident waves associated with a focalization process. Effects of the finite thickness and of the finite width of a PC slab on these three phenomena are analyzed numerically. Section 3 presents the experimental setup and the results of transmission spectra of acoustic waves through a PC slab. Agreements and discrepancies between theoretical and experimental results are discussed. Section 4 reports on a perceptual analysis of the PC slab. Focus is made on how the different phenomena studied in the two previous sections can be perceived by a naive listener. In order to achieve this goal, a detailed numerical analysis of the psychoacoustic feature called “loudness” is conducted based on impulse responses obtained in different configurations (free field/FF, PC, free-standing wall/FS). Additional perceptual tests are performed to evaluate the efficiency of

the panel in terms of perceived sound intensity. Finally, the main results of this study are summarized in the conclusion and the possibility of designing an efficient sound barrier based on the considered PC is discussed.

## 2 Description of the structure and theoretical results

### 2.1 Description of the structure

The structure under interest is a PC composed of hard solid cylinders of radius  $r = 0.05$  m arranged according to a triangular lattice with lattice parameter  $a = 0.12$  m (Fig. 1a). The structure has not been designed to present an optimal band gap in a large frequency range but to exhibit three different phenomena in the audible frequency range for further analysis with perceptual tests. These three phenomena are (a) a band gap at normal incidence ( $BG0^\circ$ ) in a specific frequency range, (b) an ABG in another specific frequency range and (c) a frequency range where negative refraction occurs.

### 2.2 Dispersion curves

To analyze wave propagation in the PC, the dispersion curves are computed with the FEM using the ATILA software [11]. Since the cylinders are assumed uniform and infinite along their axis, only a bi-dimensional mesh in the  $xy$ -plane is used. First, a single scatterer inside a unit cell with periodic boundary conditions applied on its faces is considered [12]. Quadratic interpolation elements are considered in the computation. Moreover, the cylinders are supposed to be rigid i.e. acoustic waves cannot propagate inside the cylinders, and they are placed in air considered at 20 C, assumed as a non-viscous, lossless medium. Density

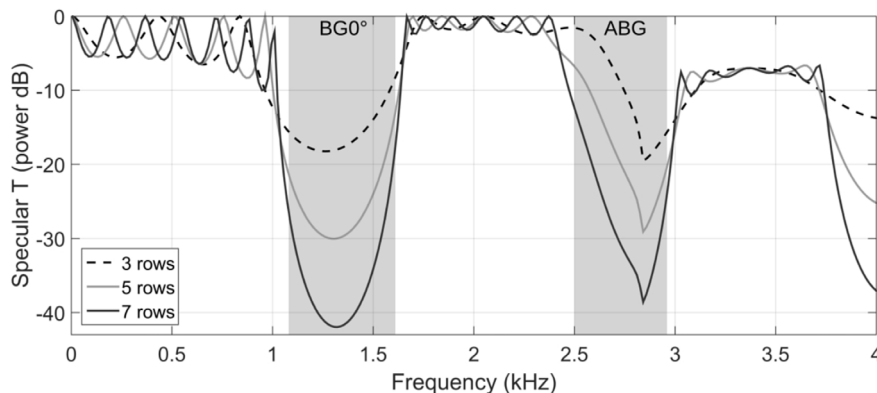


**Figure 2.** PC slab of infinite width (along  $x$ ) and finite thickness (along  $y$ ) under normal incidence, for different thickness values. Transmission coefficient for the specular beam (0, “specular T”). The gray areas indicate the two band gaps observed on the dispersion curves (referred to as  $BG0^\circ$  and ABG).

and sound velocity in air are  $\rho_{\text{air}} = 1.3 \text{ kg}\cdot\text{m}^{-3}$  and  $c_{\text{air}} = 339 \text{ m}\cdot\text{s}^{-1}$ , respectively. To draw the dispersion curves (Fig. 1b), i.e. the diagram representing the eigenmode frequencies of the PC that are associated with a specific wave vector, versus the wave vector, it is not necessary to consider all the wave vectors but it is sufficient to span a relatively small range of wave vectors covering the edges of the irreducible Brillouin zone (IBZ) (see [3]). For the triangular array of cylinders presented in this article, the IBZ corresponds to the  $\Gamma X$  triangle where the coordinates of points  $\Gamma$ ,  $J$  and  $X$  in an orthonormal basis of the  $xy$ -plane are  $\Gamma : \frac{2\pi}{a}(0, 0)$ ,  $J : \frac{2\pi}{a}(\frac{1}{3}, \frac{1}{\sqrt{3}})$ , and  $X : \frac{2\pi}{a}(0, \frac{1}{\sqrt{3}})$ . Consequently, the  $\Gamma X$  direction corresponds to wave vectors oriented along the  $y$  direction and the  $\Gamma J$  direction corresponds to wave vectors that make a  $30^\circ$  angle with the  $y$  direction (see arrows in Fig. 1a). Figure 1b shows the dispersion curves calculated for a wave vector describing the  $X \rightarrow \Gamma \rightarrow J \rightarrow X$  path of the IBZ.

Along the  $\Gamma X$  direction, a band gap is observed for frequencies between 1080 Hz and 1610 Hz (in dark gray in Fig. 1b). The band gap is not absolute since modes can propagate in this frequency range along the  $\Gamma J$  and  $JX$  directions of propagation. For the experiments, the PC will be oriented so that the  $\Gamma X$  direction corresponds to the normal incidence direction. At higher frequencies, from 1610 Hz to 2500 Hz, the dispersion curves exhibit branches with a negative slope. The dashed straight lines corresponding to the sound velocity in air cross these branches at two slightly different frequencies along the principal directions of propagation, namely 1620 Hz along  $\Gamma X$  and 1550 Hz along  $\Gamma J$ . This rather small difference in frequency indicates a slight anisotropy of the acoustic wave propagation through the PC which may influence its focalization properties. Indeed, perfect focalization by a PC slab requires the “All Angle Negative Refraction” criterion [13] to be satisfied, i.e. the phase velocities in the PC and external air medium must match for all angles of incidence. This criterion is not strictly satisfied in our PC, but some focalization effect can still be expected. At even higher frequencies, in the range

from 2500 Hz to 2960 Hz, no propagation mode exists. In this ABG propagation of acoustic waves is forbidden whatever the incident direction.

## 2.3 Harmonic analysis of the PC slab in free-field

### 2.3.1 PC slab of infinite width and finite thickness

To verify that the dispersion properties of the infinite PC can be easily evidenced for a finite PC of practical dimensions, several preliminary numerical tests are conducted. First, the transmission spectrum under normal incidence ( $\Gamma X$  direction) is calculated for a PC slab of infinite width along  $x$  but of finite thickness along  $y$  (Fig. 2). In the FEM simulation, the infinite width is modeled using periodic boundary conditions on the sides of the domain. Thicknesses corresponding to 3, 5 and 7 rows of scatterers are tested here. It can be seen that the transmission dips corresponding to the PC band gaps are already well defined for 5 rows, with frequency limits close to those of the dispersion curves, and transmission levels going down to  $-30$  dB.

### 2.3.2 PC slab of finite width and finite thickness

To facilitate fabrication, the width of the PC slab should be limited as much as possible. Therefore, in this subsection, the influence of a limited width is studied to investigate if the expected effects ( $BG0^\circ$ , focalization and ABG) are still observed. The numerical simulation is performed on a phononic crystal of finite spatial extent, made of 57 cylinders (5 rows of alternatively 11 and 12 cylinders), as depicted in Figure 3. The width and the thickness of the slab are approximately 1.42 and 0.52 m, respectively. Again, the calculation is performed using the FEM [11] and the 2D mesh includes the slab and a large region of air around the slab, including non-reflecting elements at the external boundary of the mesh. An ideal omnidirectional point source is placed 0.10 m away from the center of the first row of cylinders, and laterally centered, so that it stands in front of a cylinder. Figure 3 presents the pressure field around the acoustic barrier for three different

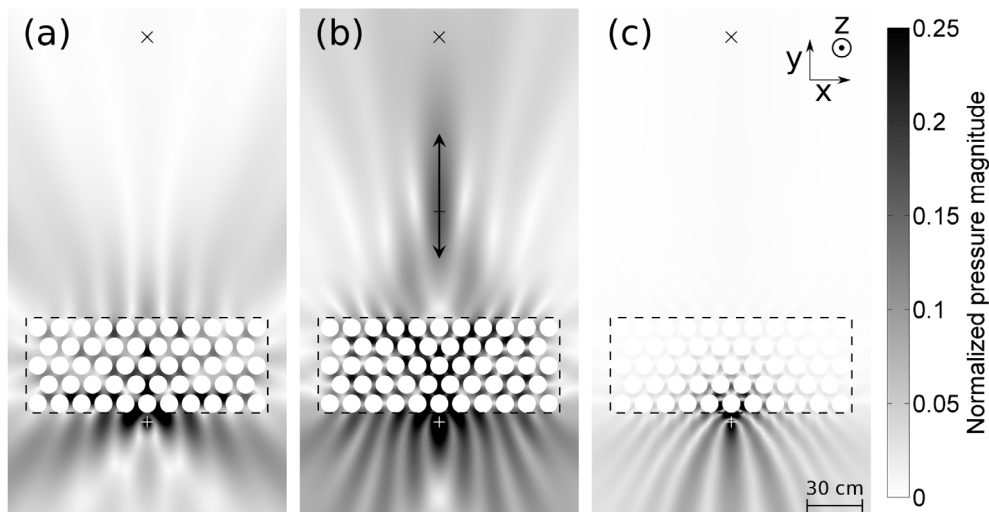


**Figure 3.** Simulated normalized pressure field for (a) 1300 Hz (BG0°), (b) 1700 Hz (negative refraction and focalization effect) and (c) 2700 Hz (ABG). Pressure level at the point source (marked by a white “+” sign) is normalized to 1 Pa. Regions where the grayscale is saturated (i.e. normalized pressure magnitude is above 0.25) are shown in black. The position of the pseudo-listener (not used in the simulation, only shown here as a guide for the reader) is indicated with a black “x” sign, and the dashed rectangle indicates the position of the wall for the FS simulation. The arrow in panel b denotes the extension of the focalization region, and the horizontal bar crossing the arrow is vertically aligned with the center of the region, i.e. the point of maximal pressure.

frequencies: 1300, 1700 and 2700 Hz, with the same gray scale. Each figure shows one phenomenon described in Section 2.2.

Figure 3a shows the pressure field at 1300 Hz, a frequency that falls in the range of the acoustic band gap at normal incidence (BG0°). As expected, due to the omnidirectional nature of the sound source, it is observed that the acoustic pressure behind the PC slab is relatively low along the  $y$  axis (reaching 0.5% of the source pressure level at 1.5 m, instead of 3.86% when the slab is absent, i.e. a 17.7 dB insertion loss), whereas it increases in the oblique directions. This indicates that waves impinging the PC with oblique incidences may propagate through the PC whereas those with normal incidence are stopped, in agreement with the non-absolute feature of the band gap. This simulation result shows that even with an omnidirectional source, the impact of the directional band gap on the sound levels behind the panel is quite significant. Figure 3b shows the source image due to the negative refraction and the focalization effect at 1700 Hz. This frequency corresponds to the frequency for which the pressure field behind the PC slab exhibits its maximal value. Consequently one may expect the most important focalization effect at this frequency. To precisely locate the image point inside the focalization area, the pressure field along a vertical line has been analyzed. This line is parallel to the  $y$  axis (see Fig. 1a) and passes through the sound source and through the focalization area. The results depicted in Figure 3b show that the acoustic pressure is maximal at 0.58 m (reaching 16% of the source pressure level), and the focalization area extends from 0.32 m to 1.01 m behind the slab (these distances denoting the positions at which the pressure falls 3 dB below the maximal acoustic pressure). The distance between the sound source and the local maximum of

pressure is then close to twice the slab thickness (1.15 m instead of 1.04 m) indicating that the all-angles negative refraction criterion is nearly satisfied [5]. Figure 3b shows that the focalization process is creating a mirror-source on the other side of the panel. In Figure 3c, the frequency, 2700 Hz, falls in the ABG and the calculated pressure is accordingly very low in all directions behind the slab. For instance, a pressure level equal to 0.4% of the source value is observed at 1.5 m on the  $y$ -axis, instead of 3.14% with the slab removed, corresponding to a 17.9 dB insertion loss. One may conclude that the main features that were expected from the band structure of the infinite PC are well recovered when considering a PC slab of finite width and thickness dimensions. The number of cylinders considered in each one of these directions is large enough.

### 3 Experimental study

#### 3.1 Experimental setup

To validate the theoretical predictions obtained with the FEM, an experiment is performed on a PC slab, with the aim of measuring its impulse response. The slab described in Section 2.3 is manufactured, with exactly the same geometrical characteristics but with hollow cylinders rather than filled ones (57 hollow cylinders arranged in a triangular lattice: 5 rows of 11/12 cylinders, total width = 1.4 m, total thickness = 0.5 m). The hollow cylinders are made of PVC (outer radius  $r = 0.05$  m, tube thickness = 0.002 m). It has been shown that the choice of tubes, i.e. hollow cylinders rather than filled cylinders, does not influence the experimental results for audible frequencies [14] and allows us to make a lighter experimental structure. The tubes are 2 m long and are fixed at one end on a large plywood plate, while

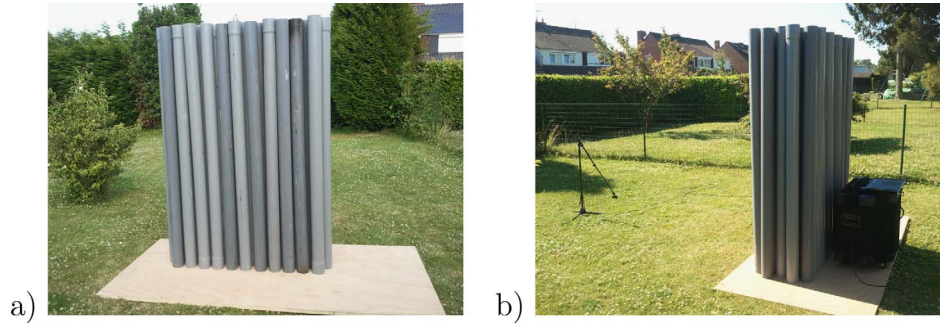


**Figure 4.** Picture of the PC-based noise barrier (a). Outdoor, free-field measurement setup (b), with the position of the microphone stand (left) and the source (right).

the other end remains free (Fig. 4a). The slab is placed in a peri-urban, not dense, residential area, and the measurements are made during the middle of a workday, ensuring a calm, low-level acoustic environment (measured background noise level: 42 dB(A)). The length of the tubes has been chosen to be much larger than the periodicity of the array and the incident wavelength to validate the assumption of cylinders of infinite extent along their axis.

A 0.61 m-wide Gallien Krueger 410RBH loudspeaker, amplified by a B&K type 2716 audio power amplifier connected to a Roland Quad Capture sound card is employed to produce the incoming acoustic wave. The source is placed 0.10 m away from the slab, whereas the microphone is placed 1.5 m behind it (see Fig. 4b for a picture of the experimental setup). The transmitted wave is recorded by a Sennheiser MKE2-P-C microphone connected to the same sound card. No dummy head for binaural recording is employed. A sampling frequency of 48 kHz is used. The incoming signal is a logarithmic swept-sine of 5 s between 100 and 4000 Hz. Repeating the sweep excitation 10 times allowed us to increase the signal-to-noise ratio from 22 dB to 32 dB.

### 3.2 Experimental results

The analysis is presented through the insertion loss (IL) defined as the ratio between the pressure levels without and with the PC slab. Thus, a positive value corresponds to a pressure level reduction. Since the loudspeaker is 0.61 m wide while the numerical computation considers a point sound source, the theoretical curve is an average of 62 computations where the point source was moved from  $x = -0.305$  m to  $x = +0.305$  m by 0.01 m steps stands for the center of the front side of the PC slab). This is meant as an attempt to take into account the width (along horizontal axis  $x$ ) of the source in the 2D simulation: Our hypothesis is that the directivity pattern of the loudspeaker is a combination of 62 ideal cylindrical sources. Figure 5 compares the measured and simulated IL spectra. Predictions and measurements present an overall agreement especially above 2500 Hz. In fact, the source is placed very close to the PC slab and the height of the tubes (2 m) is much greater than the wavelength in the frequency range of interest. Therefore, an array of infinite cylinders along

the vertical dimension  $z$  is considered in the simulation process. Also, the numerical simulations assume an ideal cylindrical source (i.e., infinite in the vertical direction). The IL stays in the 15–30 dB range in the BG0° (from 1080 Hz to 1610 Hz) and in the 20–30 dB range in the ABG (from 2500 Hz to 2960 Hz). In the intermediate frequency range from 1610 Hz to 2500 Hz, one notes that the calculated IL remains nearly constant (around zero), while the measured IL exhibits a dip at approximately 2200 Hz. This dip, which occurs in the negative refraction band, corresponds to an amplification of the measured output signal. One may attribute this apparent discrepancy between experiments and simulation to the approximate modeling of the sound source in the calculations (sum of 62 point sources vs. large experimental source). However, the experimental spectrum shows that, in the frequency range of the negative refraction, the pressure at 1.5 m from the panel is higher with the PC due to the presence of the “mirror-source” on the other side of the panel. The negative refraction leads to a focalization of the output signal that may lead to the perception of a source closer to the listener. This is in agreement with the observations made by Spiouzas et al. [8, 9], speaking of an “auditory illusion of proximity of the sound source”.

## 4 Perceptual analysis

In this section, it is tested whether the modifications brought by the PC lead to significant differences from an auditory perspective. First, Moore-Glasberg loudness [15, 16] is analyzed. Then perceptual tests are performed on human listeners. All results reported in this section use data obtained from FEM simulations.

### 4.1 Data

The simulation conducted in Section 2.3.2 is repeated with a pseudo-listener placed at 1.50 m behind the PC sample, i.e. about 0.90 m beyond the image point (see the black cross on top of each panel in Fig. 3c). A rigid cylinder with a 0.10 m radius is used as a model of the listener. The sound source (in the simulation, no loudspeaker is used as in Sect. 3, a point source is used instead) and the listener are

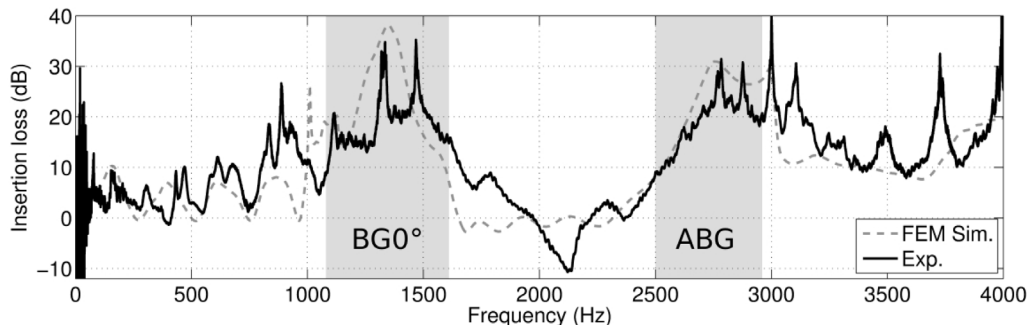


**Figure 5.** Measured and simulated insertion loss introduced by the PC-based noise barrier. The simulated results correspond to the sum of 62 simulations, each one corresponding to a point source which position moves from  $x = -0.305$  m to  $x = +0.305$  m, with a 0.01 m step. The measurement point is located 1.5 m behind the slab. Gray shaded areas indicate band gaps:  $BG0^\circ$  between 1080 and 1610 Hz, ABG between 2500 and 2960 Hz.

placed on each side of the structure. To analyze the effects of the PC slab on the propagation of audible acoustic waves, three types of simulations are performed: (a) in free-field (FF), i.e. when there is no obstacle between the sound source and the pseudo-listener, (b) with the PC slab (see its description in Sect. 3.1) and (c) with the free-standing (FS) wall, or barrier (considered as rigid) that has the same thickness and width as the PC slab (width 1.42 m and thickness 0.52 m).

A harmonic analysis is performed in the frequency range from 7.81 Hz to 4000 Hz, with a step of 3.9 Hz (i.e. 1024 points). Complex acoustic pressure is calculated on each “ear” of the pseudo-listener (left and right sides of the cylinder), to simulate the acoustic signals received at the ear reference point (ERP) according to the classification of the International Telecommunication Union (ITU) [17]. An inverse Fourier transform is applied to obtain the 256 ms impulse response for each of the three sound scenes FF, PC and FS (with a sampling frequency of 8000 Hz).

Section 4.2 describes how the numerical impulse responses are processed for the detailed analysis of the frequency modifications introduced by the PC slab on the perceived sound level, or loudness.

#### 4.2 A psychoacoustic feature: Moore-Glasberg loudness

From Spiouzas et al. [8, 9], one may expect that a PC introduces both spectral and sound level modifications on an acoustic signal emitted by a sound source. To estimate the potentially frequency-dependent effect of the PC on the perceived sound level, the numerical, full-band impulse responses of each configuration (FF, FS, PC) are convolved with third-octave noises (i.e., white noise filtered with 2nd-order Butterworth filters of center frequencies corresponding to the classical third-octave bands). The resulting signals are resampled to 48 kHz, and the Moore-Glasberg loudness is computed using Matlab’s “Audio Toolbox”. This model takes into account the frequency masking effect and is optimized for signals such as the third-octave noises described above. The sound pressure level at the pseudo-listener is normalized to 66 dB SPL (Sound Pressure Level) for the third-octave band of central frequency 1000 Hz in

free-field condition (FF sound scene). Figure 6 presents the estimated loudness (at the right ear of the pseudo-listener, assuming perfect symmetry of the setup, i.e. no difference is made between right and left ear) of the 15 third-octave bands with central frequencies 125–3150 Hz for the 3 sound scenes (FF, PC and FS). Note that it was preferred to use standard third-octave bands, with the result that these bands are not aligned with the band gap and negative refraction frequencies (in particular no band centered within the ABG). The FS sound scene clearly shows lower loudness values, which is expected for a free-standing wall placed between the sound source and the listener. In the frequency range of the first band gap (near 1250 Hz- $BG0^\circ$ ), as expected the loudness for the PC sample is lower than the loudness for the FF sound scene. In this frequency band, the loudness drops and then reaches approximately the same level as that of the FS wall. The noise control enabled by a slab made of this specific PC is similar to a free-standing rigid wall for frequencies close to the first band gap. Near 2000 Hz (frequency range of the negative refraction and focalization effect), the loudness for the PC barrier increases and is higher than the loudness for the FF and FS scenes. The slab acts as an artificial amplifier of the loudness due to the focalization process. In contrast with the first band gap ( $BG0^\circ$ ), the influence of the second one (ABG) on the loudness is less obvious. This is mainly due to the fact that, in this frequency range, the width of the band gap is more limited with respect to the third-octave bandwidths. In practice, the 2500–2960 Hz band gap is only in partial overlap with the bands centered on 2500 Hz (2239–2818 Hz range) and 3150 Hz (2818–3548 Hz range). Moreover, for the very last third-octave band, the acoustic field is further modified due to the apparition of diffraction grating effects. Indeed, since the output interface of the PC slab is a periodic array of scatterers with a periodicity  $a = 12$  cm, new outgoing waves start to appear above  $f = c_{\text{air}}/a = 2825$  Hz and outside the ABG, along with significant modifications of the slab near-field.

Finally, above 2500 Hz, which corresponds to the ABG, the loudness for PC drops again.

In conclusion, a slab made of this specific PC shows noise control properties that are similar to a free-standing

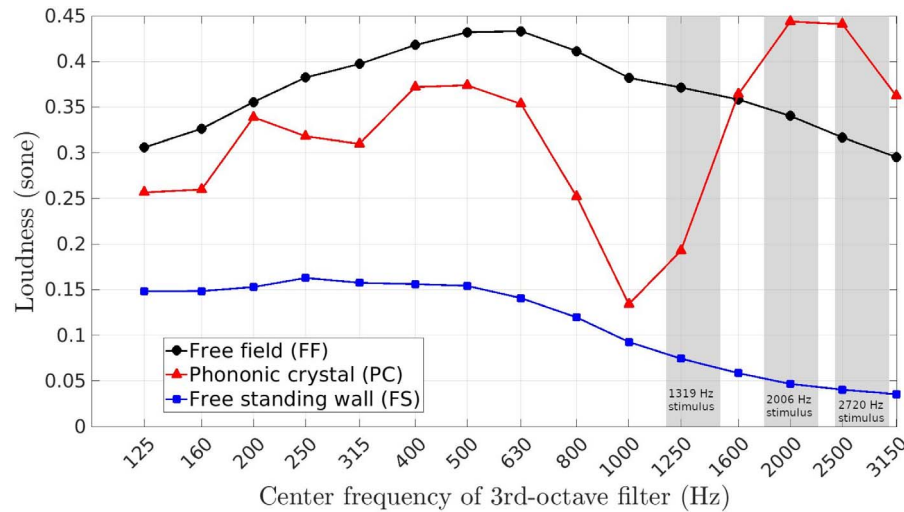


**Figure 6.** Estimated loudness at the right ear of the pseudo-listener of the 15 third-octave band white noises with central frequencies 125–3150 Hz for the FF, PC and FS sound scenes. Gray shaded areas show the frequency bandwidth of the stimuli defined in Section 4.3, centered around 1319, 2006, and 2720 Hz (width of 1/3 octave each).

rigid wall for frequencies close to the band gaps, and it introduces an artificial amplification in the frequency range of the negative refraction phenomenon, as an illusion on the source position. Note that the loudness is computed on normalized third-octave bands that don't perfectly match the frequency characteristics of the PC: as a result, in Figure 6 the visible effect of the PC on loudness augmentation or reduction may therefore be underestimated. Sections 4.3 and 4.4 describe a perceptual test that aims at verifying if these loudness variations are perceptible.

### 4.3 Design of the perceptual test

The computation of the psychoacoustic loudness (Sects. 4.2 and Fig. 6) exhibits clear differences and similarities between the PC and the other two configurations (FF and FS). To assess whether these differences are actually perceived by human listeners, a listening test is conducted, with twenty-five participants participating in a pair comparison test<sup>1</sup>. The test takes place in a quiet room, and the test interface is implemented using Matlab on a HP laptop with an external Roland Quad Capture sound card. The stimuli are played over Prodipe Pro880 headphones delivering a level of 73 dB at the position of the ear.

As differences in the computed loudness between the configurations (FF, FS, PC) are observed in the frequency range of the typical phenomena expected from a PC, the perceptual test focuses on these frequency ranges. Nine stimuli are produced from the convolution of three third-octave noises centered around frequencies 1319, 2006, and 2720 Hz, respectively, with the impulse responses of the FF, FS, and PC configurations. These frequencies are the center (in the sense of the geometric mean) of the frequency

bands of interest: 1080–1610 Hz for the BG0°, 1610–2500 Hz for the focalization, and 2500–2960 Hz for the ABG.

The order of presentation of stimuli is randomized. The comparison is made between configurations (PC, FS, FF), not between center frequencies, e.g. a PC sound centered at 1319 Hz is always compared to a sound centered at 1319 Hz, from a PC, FS, or FF configuration. For a given pair, the two possible combinations (e.g. FS/PC then PC/FS) are used in order to assess the consistency of the listener's answers, and the pair of identical stimuli (e.g. PC/PC) is also consistently assessed.

For each pair of stimuli, the listener is asked to listen to both sounds played successively and to judge on a 7-point scale whether the second sound is louder or softer than the first one. The question is the following: “With respect to the first one, the second sound seemed to you...”.<sup>2</sup> The scale is labeled with the following phrases that are to be chosen to conclude the question: “much softer”, “softer”, “slightly softer”, “identical”, “slightly louder”, “louder”, “much louder”. These labels are reported in Figures 7 and 8, and are converted to integer numbers from -3 to 3 for the statistical analysis.

### 4.4 Statistical analysis of the perceptual test

Figures 7a–7c show the answers of all participants, for the noises centered at 1319, 2006, and 2720 Hz, respectively. Distributions of perceptual answers (7-point scale) are grouped according to the order of presentation.

The Lilliefors [18] test for normality is performed on each distribution, i.e., on each 25-long vectors of loudness comparison judgement corresponding to each noise (center frequency 1319, 2006, or 2720 Hz) and each combination of

<sup>1</sup> The work presented in this article complies with the principles of the Declaration of Helsinki, published by the World Medical Association. All participants provided informed, written consent before taking part in the experiment.

<sup>2</sup> Instructions as well as labels of the scale are an English translation of the original French wording.



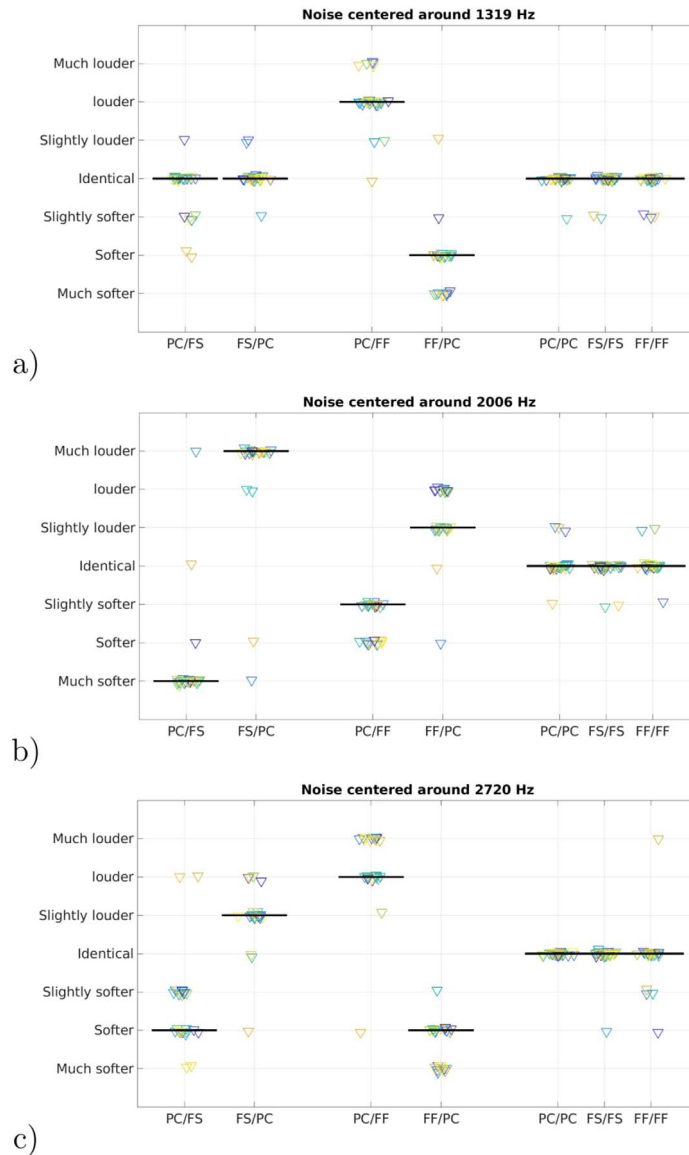


**Figure 7.** Answers in the perceptual test, noise centered around 1319 Hz (a), 2006 Hz (b), and 2720 Hz (c); for the comparison between PC/FS, FS/PC, PC/FF, and FF/PC configurations, where the first configuration in each pair corresponds to the first presented stimulus. The second configuration is rated on the scale in comparison to the first one, i.e. PC/FS is the comparison of FS with respect to PC. The triangles indicate individual ratings (ratings from the same participant have the same color). The horizontal bars represent the median of each distribution. For ease of reading reasons, small horizontal and vertical offsets are used for displaying the individual answers as black triangles (each answer originally is an integer number between  $-3$  and  $3$ ). Answers for stimuli pairs made of identical stimuli (PC/PC, FS/FS, FF/FF) are also shown for checking consistency.

two configurations (PC/FF, FF/PC, PC/FS, FS/PC). For all distributions, the hypothesis of a normal (Gaussian) distribution was rejected at the  $\alpha = 0.01$  significance level, with all  $p$ -values less than 0.001. Because no distribution can be said to be normal, Figures 7a–7c do not show mean and standard deviation but instead all single answers and the median value. Another consequence is that, in order to check if the differences seen across distributions have a statistical significance (i.e., are likely to hold true in a more general case), we must use non-parametric statistical tests, e.g. Kruskal-Wallis [19], Wilcoxon signed-rank test, or Wilcoxon rank sum test [20], comparing the median values

(instead of the mean values) of the distributions to a  $\chi^2$  distribution. Note that in the following, a  $p$ -value threshold of 0.01 is chosen for deciding on the significance of the statistical tests. This choice minimizes the probability of type-1 errors, i.e. rejecting an  $H_0$  hypothesis even if it is true [21]. The  $p$ -value is the largest probability of obtaining the observed distribution if the null hypothesis is true. In the case of the Kruskal-Wallis and Wilcoxon rank sum tests, a  $p$ -value of 0.01 therefore indicates that the distributions have a probability less than 1% to come from a unique distribution (the so-called null hypothesis being here that the tested distributions come from a unique distribution).

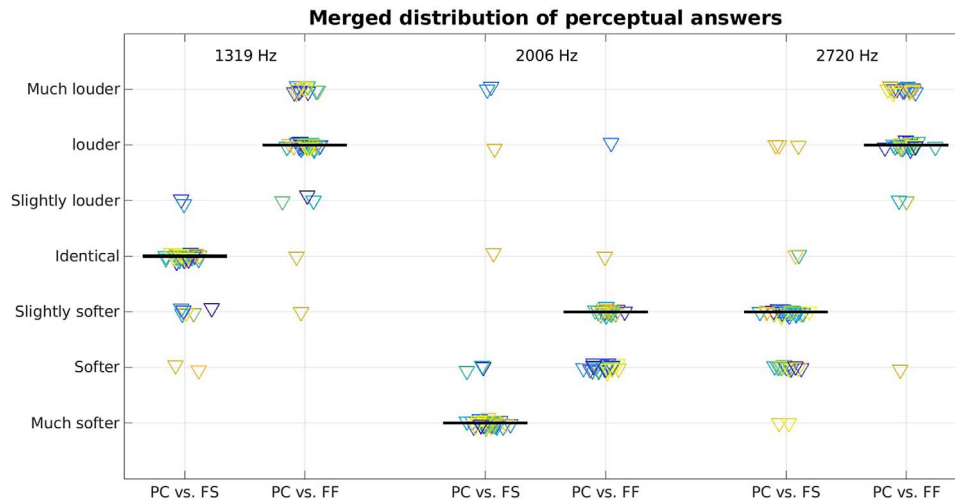


**Figure 8.** Answers in the perceptual test, merged by “symmetrical” pairs (e.g. PC/FS and FS/PC merged together into “PC vs. FS”). As in Figure 1, the second configuration is rated on the scale in comparison to the first one, i.e. “PC vs. FS” is the comparison of FS with respect to PC. Only pairs concerning the PC configuration are shown. Distributions are separated with respect to frequency band of interest: 1319 (left), 2006 (center), and 2720 Hz (right). The triangles indicate individual ratings (ratings from the same participant have the same color). The horizontal bars represent the median of each distribution. For ease of reading reasons, small horizontal and vertical offsets are used for displaying the individual answers as black triangles (each answer originally is an integer number between  $-3$  and  $3$ ).

In the case of the Wilcoxon signed-rank test, a  $p$ -value of 0.01 indicates that the distribution has a probability less than 1% to have a median equal to 0.

In Figures 7a–7c, identical stimuli seem to be consistently assessed as “identical” (see right-hand side of Figs. 7a–7c, evaluation of PC/PC, FS/FS, and FF/FF pairs). For each distribution of answers involving a pair of identical stimuli (e.g. PC/PC at 1319, 2006, and 2720 Hz, and similarly for FS/FS, and FF/FF), a Wilcoxon signed-rank test fails to reject the hypothesis that the distribution has a median different from 0 (all  $p$ -values higher than 0.25<sup>3</sup>). This means that it can not be shown that physically identical stimuli are perceived as different: the participants’ evaluation can be said to be “consistent”.

A further check of the data is done about the effect of the order of presentation in pairs of stimuli. Figures 7a–7c show that similar effects are obtained for different orders of presentation, e.g. at 2006 Hz (Fig. 7b), FS sound stimulus is perceived as “much softer” than PC stimulus, and PC sound stimulus is symmetrically perceived as “much louder” than FS stimulus. A double-sided Wilcoxon rank sum test is conducted for each “symmetrical” pair involving the PC configuration (because the article focuses on the differences brought by this very configuration): PC/FS and FS/PC at 1319 Hz, PC/FF and FF/PC at 1319 Hz, and so on with frequencies 2006 and 2720 Hz. In order to compare the pairs, care was taken to reverse the sign of the values in the second distribution of each pair. For each of these

pairs, the test failed to reject the hypothesis that the two distributions of the pair have the same median (all  $p$ -values higher than 0.01)<sup>4</sup>. This means that it is possible to merge each pair of “symmetrical” distributions into a single distribution, e.g. at a given frequency (1319, 2006, or 2720 Hz), PC/FS and FS/PC (having 25 points/evaluations each) are merged into a single 50-point distribution that we may call “PC vs. FS”, provided the sign of evaluations in the distribution FS/PC is reversed. These merged distributions are shown in Figure 8.

In rejecting the hypothesis that each of the distributions in Figure 8 has a median equal to 0 (all  $p$ -values lower than  $4.84 \times 10^{-7}$ ; except for distribution “PC vs. FS” at 1319 Hz, for which the hypothesis fails to be rejected,  $p = 0.07$ ), a Wilcoxon signed-rank test shows that, with the chosen statistical power, there is no apparent loudness difference between PC and FS at 1319 Hz, and that all other pairs of merged distributions appear to be perceived as not equally loud. The BG0° centered around 1319 Hz lowers the energy of the sound waves in this frequency band: therefore a) it makes the PC act in a similar way as a rigid wall (FS), and b) it decreases the sound energy more than a free-field propagation (FF). This is consistent with the results from the computation of the psychoacoustic loudness (Sect. 4.2): at BG0°, the loudness in the PC configuration drops to reach values obtained in the FS configuration, which are much lower than the values obtained in the FF configuration. This means that due to the BG0°, the sound

<sup>3</sup>  $p = 1, p = 0.5, p = 0.25, p = 0.625, p = 0.5, p = 1, p = 1, p = 1,$  and  $p = 0.5625$  respectively for PC/PC at 1319 Hz, FS/FS at 1319 Hz, FF/FF at 1319 Hz, PC/PC at 2006 Hz, FS/FS at 2006 Hz, FF/FF at 2006 Hz, PC/PC at 2720 Hz, FS/FS at 2720 Hz, and FF/FF at 2720 Hz.

<sup>4</sup>  $p = 0.2363, p = 0.1684, p = 0.7660, p = 0.7114, p = 0.9305,$   $p = 0.0159,$  and  $z = -1.1843, z = -1.3772, z = -0.2976,$   $z = -0.3699, z = 0.0872, z = -2.4119,$  respectively for PC/FF and FF/PC at 1319 Hz, PC/FS and FS/PC at 1319 Hz, PC/FF and FF/PC at 2006 Hz, PC/FS and FS/PC at 2006 Hz, PC/FF and FF/PC at 2720 Hz, PC/FS and FS/PC at 2720 Hz.

is well attenuated, but in terms of sonic insulation the PC is not more efficient than the FS.

The focalization band centered around 2006 Hz has the effect of increasing the energy of the sound waves, therefore it increases the perceived loudness in the PC case in comparison with the FS and FF. This is, again, consistent with the computed loudness values that are higher for the PC case. One may anticipate that, while the observation is made rather far from the focal point, the focalization process occurs, and noise is perceived as louder due to the presence of the “mirror-source” on the other side of the panel (see Sect. 2.3.2).

The ABG centered around 2720 Hz shows the same phenomenon as the BG0°: expectedly, the PC-filtered sound is perceived as softer than the sound in the FF condition, and the FS sound stimulus is perceived as “slightly softer” than the PC one at 2720 Hz. As regards the link with computed loudness, note that Figure 6 shows higher loudness values for the PC than for FF at normalized third-octave band frequencies 2500 and 3150 Hz. The fact that these frequency bands don’t match the frequency of the ABG (whereas the center frequencies of the BG0° and of the focalization band are quite close to the normalized third-octave frequencies) might be a reason for the discrepancy between computed and perceived loudness. Nevertheless, the sound attenuation is also clearly perceived as higher in the FS configuration compared to the PC one: Figure 6 indeed shows much lower loudness values in the FS case.

The effect of the PC, compared to FS and FF configurations, can also be analyzed across frequencies. The non-parametric equivalent to analysis of variance (ANOVA), the Kruskal-Wallis test, is performed to compare the “PC vs. FS” distributions at 1319, 2006, and 2720 Hz (i.e., with center frequency as a factor). It indicates that there are significant differences in the “PC vs. FS” rating across frequencies ( $\chi^2 = 91.27$ ,  $p = 1.52 \times 10^{-20}$ , 2 degrees of freedom). The Kruskal-Wallis test only reveals if there are differences in the considered distributions, but doesn’t distinguish which distributions are significantly different from which. Therefore, a post-hoc multiple comparison test (Matlab’s multcompare function, with Bonferroni correction) is performed on the pairs of distributions “PC vs. FS”. The test indicates that each “PC vs. FS” distribution is significantly different from the other two ( $p < 10^{-4}$  in each case). It confirms previous results: a) at the center frequency of the BG0° (1319 Hz), the PC acts as would a rigid wall (FS), i.e. lowering the perceived loudness by the same amount; b) at the center frequency of the focalization effect, the PC raises the perceived loudness to such an extent that the rigid wall sound stimulus sounds “much softer”; and c) at the center frequency of the ABG (2720 Hz), the PC attenuates the sound a bit less than the rigid wall, making the stimulus of the latter condition sound “slightly softer” than that of the former condition.

Similarly, a Kruskal-Wallis test is performed to compare the “PC vs. FF” distributions at 1319, 2006, and 2720 Hz. It indicates that there are significant differences in the “PC vs. FF” rating across frequencies ( $\chi^2 = 101.33$ ,  $p = 9.93 \times 10^{-23}$ , 2 degrees of freedom). Post-hoc multiple comparison

(Bonferroni corrected) indicate that the “PC vs. FF” distribution at 2006 Hz is significantly different from the other two ( $p = 0.82$ ; the other two pairs showing  $p < 10^{-4}$ ). This confirms that the same tendency to judge FF sound stimuli as louder than PC ones exists at 1319 and 2720 Hz: the band gap phenomenon is responsible for a sound attenuation that is perceptible. The frequency band of the focalization effect (2006 Hz) significantly differs in terms of perceived loudness difference between PC and FF: again, the focalization effect induces a loudness enhancement that makes the sound louder than in a free-field (FF) configuration.

## 5 Conclusion

The PC designed for this study presents three different characteristics in the audible frequency range: a first band gap at normal incidence in the frequency range 1080–1610 Hz, negative refraction in the range 1610–2500 Hz, and an ABG in the range 2500–2960 Hz. These three effects are analyzed theoretically with the help of FEM simulations and experimentally with a home-made manufactured PC slab of finite dimensions. The computation of Moore-Glasberg’s loudness shows that the PC slab is able to lower the loudness of a noise source in the band gaps of approximately the same level as a usual free-standing rigid wall of the same thickness, whereas the focalization phenomenon introduces an increase of the loudness for a specific frequency band, around 2000 Hz for this PC. This later phenomenon concentrates the acoustic energy behind the PC slab, i.e. on the listener side and must be alleviated if one desires to manufacture sound barriers based on PCs [22–24].

Perceptual tests on human listeners induce the same observations. In the frequency range of the band gaps, sound stimuli filtered by the PC’s impulse response are perceived as softer than stimuli resulting from a free-field propagation (FF), they also are perceived as equally (or close to equally) loud than sounds attenuated by the rigid wall (FS). In the frequency range of the focalization (negative refraction), PC sound stimuli sound louder than both FS and FF sound stimuli. This latter observation is associated with the existence of an image source behind the panel that makes the sound source appear closer to the listener, as already reported in Spiouzas and colleagues [8, 9]. Perceptually speaking, the loudness modifications induced by the PC can therefore be comparable to those induced by a rigid wall.

The structure presented in this paper has not been designed to exhibit an optimal band gap in a large frequency range but to exhibit three different phenomena in the audible frequency range, so that these phenomena can be analyzed with perceptual tests. This article provides a proof of concept about the potential efficiency of sound barriers made of phononic crystals in the audible range. As such, the structure exhibits all classical effects of PCs within the audible range, at the cost of working with limited-width frequency bands: The effect of PCs on the perception of broadband noises/sounds needs further investigation.

Further studies may be performed to investigate an acoustic screen made of several juxtaposed PCs in order to broaden the frequency range where sound is attenuated. Perceptual tests with more natural sounds (e.g., broadband noises, voice stimuli) may then be performed to evaluate the efficiency of such screens. Also, the perceptual effect of a noise stimulus whose frequency range encompasses several of the typical bands of the PC is worth investigating, e.g. for assessing the combined effect of band gaps and focalization on broadband sources, and their possible interaction with psychoacoustical phenomena such as critical bands and equal loudness contours. Furthermore, noise barriers made of rigid solid bulkheads are heavy and are basically continuous walls that have a negative visual impact, reduce sunlight for the surrounding residents, and have a significant resistance to the flow of air. For these reasons, discontinuous sound barriers made of isolated scatterers could also be considered, even in configurations where they do not offer superior performance.

## Acknowledgments

The authors would like to thank Quentin Souron and Gérard Haw for their help during the auditory tests and the manufacturing process of the PC structure.

## Conflict of interest

The authors declare that they have no conflict of interest in relation to this article.

## References

1. M.M. Sigalas, E.N. Economou: Attenuation of multiple-scattered sound. *Europhysics Letters* 36 (1996) 241–246.
2. J.V. Sánchez-Pérez, D. Caballero, R. Martínez-Sala, C. Rubio, J. Sánchez-Dehesa, F. Meseguer, J. Llinares, F. Gálvez: Sound attenuation by a two-dimensional array of rigid cylinders. *Physical Review Letters* 80 (1998) 5325–5328.
3. P.A. Deymier (Ed.): *Acoustic metamaterials and phononic crystals*, volume 173 of Springer Series in Solid-State Sciences. Berlin, Germany: Springer, 2013.
4. H. Pichard, O. Richoux, J.-P. Groby: Experimental demonstrations in audible frequency range of band gap tunability and negative refraction in two-dimensional sonic crystal. *Journal of the Acoustical Society of America* 132 (2012) 2816–2822.
5. A. Sukhovich, B. Merheb, K. Muralidharan, J.O. Vasseur, Y. Pennec, P.A. Deymier, J.H. Page: Experimental and theoretical evidence for subwavelength imaging in phononic crystals. *Physical Review Letters* 102 (2009) 154301.
6. A.-C. Hladky-Hennion, J.O. Vasseur, G. Haw, C. Croënne, L. Haumesser, A.N. Norris: Negative refraction of acoustic waves using a foam-like metallic structure. *Applied Physics Letters* 102 (2013) 144103.
7. L. de Ryck, J. Cuenca, K. Jambrosic, C. Glorieux, M. Rychtarikova, V. Romero-Garcia, A. Cebrecos, N. Jimenez, J.-P. Groby: Perceptual evaluation of metamaterials as insulation partitions: A listening test within the cost action denorms ca15125, in Proc. ISMA2018 and USD2018, Leuven, Belgium, 2018, 1147–1162.
8. I. Spiouzas, P.E. Etchemendy, E.R. Calcagno, M.C. Eguia: Shifts in the judgement of distance to a sound source in the presence of a sonic crystal. *Proceedings of Meetings on Acoustics* 19 (2013) 050162.
9. I. Spiouzas, P.E. Etchemendy, R.O. Vergara, E.R. Calcagno, M.C. Eguia: An auditory illusion of proximity of the source induced by sonic crystals. *PLoS One* 10 (2015) e0133271.
10. V.S. Gomez, A. Alberti, I. Spiouzas, L. Salzano, O. Edelstein, M. Eguia: Tunable sonic crystals as an extension of acoustical musical instruments, in Proc. International Symposium on Musical and Room Acoustics, La Plata, Argentina. Paper number ISMRA2016–77, 2016, 1–10.
11. A.C. Hennion, R. Bossut, J.N. Decarpigny, C. Audoly: Analysis of the scattering of a plane acoustic wave by a periodic structure using the finite element method: application to compliant tube gratings. *The Journal of the Acoustical Society of America* 87 (1990) 1861–1870.
12. P. Langlet, A.-C. Hladky-Hennion, J.-N. Decarpigny: Analysis of the propagation of plane acoustic waves in passive periodic materials using the finite element method. *Journal of the Acoustical Society of America* 98 (1995) 2792.
13. Alexey Sukhovich, Li Jing, John H. Page: Negative refraction and focusing of ultrasound in two-dimensional phononic crystals. *Physical Review B* 77 (2008) 014301.
14. J.O. Vasseur, P.A. Deymier, A. Khelif, P. Lambin, B. Djafari-Rouhani, A. Akjouj, L. Dobrzynski, N. Fettouhi, J. Zemmouri: Phononic crystal with low filling fraction and absolute acoustic band gap in the audible frequency range: A theoretical and experimental study. *Physical Review E* 65 (2002) 056608.
15. International Office for Standardization, Acoustics – methods for calculating loudness – part 2: Moore-Glasberg method. International Organization for Standardization, Geneva, Switzerland, 2017.
16. B.C.J. Moore: *An Introduction to the Psychology of Hearing*, 6th edn. Brill Publishing, Leiden, The Netherlands, 2013.
17. International Telecommunication Union: Head and torso simulator for telephonometry (ITU-T Rec. P.58). Technical report, ITU, Geneva, Switzerland, 1996.
18. H. Lilliefors: On the Kolmogorov-Smirnov test for normality with mean and variance unknown. *Journal of the American Statistical Association* 62 (1967) 399–402.
19. P. McKight, J. Najab: Kruskal wallis test. In: I.B. Weiner, W.E. Craighead, Ed. *The Corsini encyclopedia of psychology*, Wiley, 2010.
20. F. Wilcoxon: Individual comparisons by ranking methods. *Biometrics Bulletin* 1 (1945) 80–83.
21. M. Maier, D. Lakens: Justify your alpha: A primer on two practical approaches. *Advances in Methods and Practices in Psychological Science* 5 (2022) 1–14.
22. A. Krynkin, O. Umnova, A. Yung Boon Chong, S. Taherzadeh, K. Attenborough: Predictions and measurements of sound transmission through a periodic array of elastic shells in air. *Journal of the Acoustical Society of America* 128 (2010) 3496–3506.
23. J. Sánchez-Dehesa, V.M. Garcia-Chocano, D. Torrent, F. Cervera, S. Cabrera, F. Simon: Noise control by sonic crystal barriers made of recycled materials. *Journal of the Acoustical Society of America* 129 (2011) 1173–1183.
24. C. Lagarrigue, J.-P. Groby, V. Tournat: Sustainable sonic crystal made of resonating bamboo rods. *Journal of the Acoustical Society of America* 133 (2013) 247–254.